Rock Mech. Rock Engng. (2002) 35 (3), 161–170
DOI 10.1007/s00603-001-0020-y

**Rock Mechanics
and Rock Engineering**
Printed in Austria

An Orthotropic Cosserat Elasto-Plastic Model for Layered Rocks

By

D. P. Adhikary and **H. Guo**

CSIRO Exploration and Mining, Kenmore, Australia

Received October 15, 2000; accepted July 30, 2001
Published online August 2, 2002

Summary

Modelling the behaviour of rock masses consisting of a large number of layers is often necessary in mining applications (e.g. coal mining). Such a modelling can be carried out in a discontinuum manner by explicit introduction of joints. When the number of rock layers is large, it is advantageous to devise a continuum-based model in which case the joints are considered to be virtually smeared across the mass. In this study, a fully elasto-plastic equivalent continuum model suitable for describing the behaviour of such layered rock masses is considered. The model is based on the Cosserat continuum theory and incorporates the moment stresses in its formulation. In contrast to the earlier Cosserat models, the possibility of rock layer plasticity is considered. The accuracy of the developed Cosserat model is verified against analytical and experimental results.

1. Introduction

Rock masses are often intersected by discontinuities, such as regular bedding planes, foliation or joints, producing a layered (foliated) structure. Layered rock masses are common in the mining environment. Simulation of excavations in layered rock masses can be carried out with a discontinuum model by explicit introduction of joints (rock layer interfaces) into a numerical formulation using either the finite element or distinct element approach (Goodman et al., 1968; Cundall, 1987).

When the number of layers to be modelled is excessively large (i.e. when the layers are thin compared to the dimensions of the engineering structures) it is advantageous to devise a continuum-based method. For the case of rock layers with bending stiffness, such a model can be formulated successfully on the basis of Cosserat theory (Cosserat and Cosserat, 1909).

The Cosserat model provides a large-scale (average) description of a layered medium. In this model, inter-layer interfaces (joints) are considered to be smeared across the mass, i.e. the effects of joints are implicit in the choice of stress-strain model formulation. An important feature of the Cosserat model is that it incorporates bending rigidity of individual layers in its formulation and this makes it different from other conventional implicit models. A distinctive advantage of the Cosserat model is that in the process of numerical modelling the problem region can be discretised with a coarser mesh (i.e. subdivided into fewer finite elements) than in explicit schemes where the size of the finite elements cannot exceed the layer thickness. Thus, in this scheme, the size of the finite elements is solely dictated by computational needs.

Such equivalent continuum models were formulated in Mühlhaus (1993) and Adhikary and Dyskin (1998) where the rock layers were assumed to be elastic. In Adhikary and Dyskin (1998), provision was made for plastic deformation along the joints only.

In this study, a fully elasto-plastic two-dimensional plane strain Cosserat model is developed, such that both joints and intact rock (rock layers) are allowed to undergo plastic deformation. The yield of both the rock matrix and the joints is defined by Mohr-Coulomb criteria with tension cut-off. In the model formulation, the deformation is assumed to be time independent and infinitesimal.

2. Theoretical Formulation

A full description of two dimensional plane strain Cosserat model with elastic rock layers was previously presented in (Adhikary and Dyskin, 1998; see also references cited there). Hence, only the plasticity formulation part will be discussed here. Using the Cartesian coordinates (x_1, x_2), the material point displacement can be defined by a translational vector (u_1, u_2) and by a rotation Ω_3. Here, axis 3 is aligned to the out of plane direction and axis 2 is perpendicular to the layers.

The two-dimensional Cosserat model has 4 non-symmetric stress components $\sigma_{11}, \sigma_{22}, \sigma_{21}, \sigma_{12}$ and two couple stresses m_{31}, m_{32}. When the rock layers are aligned in the 1-coordinate direction, the moment stress term m_{32} vanishes. The four stresses are conjugate to four deformation $\gamma_{11}, \gamma_{22}, \gamma_{21}, \gamma_{12}$ measures defined by:

$$\gamma_{ij} = \frac{\partial u_j}{\partial x_i} - \varepsilon_{3ij}\Omega_3 \tag{1}$$

and the couple stress m_{31} is conjugate to the respective curvature κ_1 defined by:

$$\kappa_1 = \frac{\partial \Omega_3}{\partial x_1}. \tag{2}$$

The elastic stress strain relationships are described by:

$$\sigma = [D_e]\boldsymbol{e}_e, \tag{3}$$

where

$$\sigma = \{\sigma_{11}, \sigma_{22}, \sigma_{21}, \sigma_{12}, m_{31}\}, \quad \boldsymbol{e} = \{\gamma_{11}, \gamma_{22}, \gamma_{21}, \gamma_{12}, \kappa_1\} \tag{4}$$

and

$$D = \begin{bmatrix} A_{11} & A_{12} & 0 & 0 & 0 \\ & A_{22} & 0 & 0 & 0 \\ & & G_{11} & G_{12} & 0 \\ & symm & & G_{22} & 0 \\ & & & & B_1 \end{bmatrix}; \tag{5}$$

here,

$$A_{11} = \frac{E}{1 - v^2 - \frac{v^2(1+v)^2}{1 - v^2 + \frac{E}{hk_n}}}, \quad A_{22} = \frac{1}{\frac{1 - v - 2v^2}{E(1-v)} + \frac{1}{hk_n}}, \quad A_{12} = \frac{v}{1-v} A_{22}, \tag{6}$$

$$\frac{1}{G_{11}} = \frac{1}{G} + \frac{1}{hk_s}, \quad G_{11} = G_{12} = G_{21}, \quad G_{22} = G_{11} + G, \tag{7}$$

and

$$B_1 = \frac{Eh^2}{12(1-v^2)} \left(\frac{G - G_{11}}{G + G_{11}} \right), \tag{8}$$

where E is the Young's modulus of the intact layer, v is the Poisson's ratio, h is the layer thickness, G is the shear modulus of the intact layer, k_n and k_s are the joint normal and shear stiffnesses.

The layer interfaces can exhibit three different modes of behaviour: (a) elastically connected with the interface normal and shear stiffness, (b) plastic with frictional sliding and (c) disconnected with tensile opening. Similarly the rock layer may either deform elastically or may sustain some plastic deformation as well. With this in mind, the rate of the deformation tensor is decomposed into elastic and plastic parts:

$$\dot{e} = \dot{e}_e + \dot{e}_p. \tag{9}$$

In a manner similar to the conventional plasticity theory the rate of plastic deformation is assumed to be equal to:

$$\dot{e}_p = \dot{\lambda} \frac{\partial g}{\partial \dot{\sigma}}, \tag{10}$$

where $\dot{\lambda}$ is the so-called plastic multiplier and g is the plastic potential function. Then the incremental elasto-plastic relationships in the general form can be expressed as usual:

$$\dot{\sigma} = \lfloor D_{ep} \rfloor \dot{e} \tag{11}$$

where, $\dot{\sigma}$ and $\dot{e}$ are the incremental stress and strain, and

$$D_{ep} = D_e - \alpha \frac{D_e \left\{ \frac{\partial g}{\partial \sigma} \right\} \left\{ \frac{\partial f}{\partial \sigma} \right\}^T D_e}{\left\{ \frac{\partial f}{\partial \sigma} \right\}^T D_e \left\{ \frac{\partial g}{\partial \sigma} \right\}}. \tag{12}$$

Here $f \leq 0$ is the yield function, g is the plastic potential and α is defined as:

$$\alpha = 1 \quad \text{if } f = 0 \text{ and } \dot{\lambda} \text{ (plastic multiplier)} > 0; \quad 0 \quad \text{if } f < 0 \text{ and/or } \dot{\lambda} \leq 0. \tag{13}$$

The course of derivation leading to Eq. (12) is exactly the same as in standard continua so it will not be discussed in detail here. Simply the yield and plastic potential functions adopted in this study will be introduced.

The yield criterions for interface sliding, f_s^{joint}, and the corresponding plastic potential function, g_s^{joint}, for a joint parallel to the 1-axis are defined as (here tension is assumed to be positive):

$$f_s^{\text{joint}} = |\sigma_{21}| + \sigma_{22} \tan \phi^{\text{joint}} - c^{\text{joint}} = 0, \quad g_s^{\text{joint}} = |\sigma_{21}| + \sigma_{22} \tan \psi^{\text{joint}} \tag{14}$$

where ϕ^{joint}, ψ^{joint} and c^{joint} designate the angle of friction, dilation angle and the cohesion of the joints respectively. Similarly, the yield criterion for the tensile opening and the corresponding plastic potential function are written as:

$$f_t^{\text{joint}} = \sigma_{22} - \sigma_{\text{ten}}^{\text{joint}} = 0, \quad g_t^{\text{joint}} = \sigma_{22}, \tag{15}$$

where $\sigma_{\text{ten}}^{\text{joint}}$ is the joint tensile strength.

Here we are dealing with asymmetric stresses and couple stresses in the rock layer. For simplicity, the rock yield function is formulated on the basis of symmetric part of the stress tensor with the incorporation of the moment stresses. In this study, the couple stress is assumed to introduce additional axial stress in the rock layer. In a beam (rock layer) subjected to a bending moment, axial stress and strain vary linearly across the depth of the section. As the bending moment is increased the yield stress is attained first at the outer fibres. Once such yield stress is attained, the rock layer could be considered broken and subsequently a zero tensile strength could be assigned. The magnitude of this bending moment in a beam can be calculated in terms of ultimate yield stress $\sigma_{\text{ten}}^{\text{rock}}$ in the following manner:

$$M^{\text{yield}} = \sigma_{\text{ten}}^{\text{rock}} bh^2/6. \tag{16}$$

Here, b is the breadth of the beam in the out of plane direction x_3 and h is the beam thickness.

The plastic couple stress can be expressed as the plastic moment per unit area as:

$$m_{31}^{\text{yield}} = M^{\text{yield}}/bh. \tag{17}$$

Equations (16) and (17) yields:

$$\sigma_{\text{ten}}^{\text{rock}} = 6m_{31}^{\text{yield}}/h. \tag{18}$$

Similar to the joint failure modes, rock matrix is assumed to fail either in tension or shear. Tensile strength of rocks is often observed to be 10 to 40 times less than the uniaxial compressive strength. Thus, when there is relatively large moment stress in the rock layer due to bending, it is most likely that the rock layers will fail in tension. When the moment stress in the rock layer is small (in the absence of layer bending) both shear and tensile failure remain a possibility and will largely be determined by the conventional stresses. In this case asymmetry in stresses will be small. Thus, in order to capture the tensile failure of the rock layer subjected to bending, the effective normal stress in the rock layer is defined by:

$$\sigma_{11}^{N} = \frac{6|m_{31}|}{h} + \sigma_{11}, \tag{19}$$

where, σ_{11} is the conventional normal stress acting along the direction of layering.

Then the rock layer yield criterion can be defined in terms of the symmetric part of the stress tensors as:

$$f_s^{\text{rock}} = (\sigma_{11}^{N} - \sigma_{22})^2 + (\sigma_{12} + \sigma_{21})^2 - ((\sigma_{11}^{N} + \sigma_{22})\sin\phi_r - 2C_r\cos\phi_r)^2 = 0 \tag{20}$$

and

$$f_t^{\text{rock}} = \sigma_{\max} - \sigma_{\text{ten}}^{\text{rock}} = 0, \quad \text{(here tension is +ve)}. \tag{21}$$

Similar to the joint plastic potential functions, the rock plastic potential functions are obtained simply by replacing rock friction angle by rock dilation angle. While formulating D_{ep}, B_1 is either made equal to zero if rock layer is yielding or made equal to $Eh^2/12(1-\nu^2)$ if joint alone is yielding. The finite element formulation of 2D Cosserat model is fully described in Mühlhaus (1993) and Adhikary and Dyskin (1998). Of course, when the bending moment vanishes (i.e. $h = 0$) the Classical continuum model is recovered.

3. Numerical Verification

Two examples will be considered here in order to verify the capability of the fully elasto-plastic Cosserat model. First of all, a simple case as shown in Fig. 1, is considered. Here 10 layers are perfectly clamped on the left-hand side and a traction τ_s is applied on the right hand side. The rock layers are assumed to have Young's modulus (E) of 10 GPa, Poisson's ratio of 0.20, thickness of 1 m, length (l) of 10 m and tensile strength ($\sigma_{\text{ten}}^{\text{rock}}$) of 0.5 MPa. The joint shear stiffness is taken to be zero. Thus the Cosserat solution should remain independent of the x_2 direction, which allows analytical verification of the Cosserat result on the basis of beam theory.

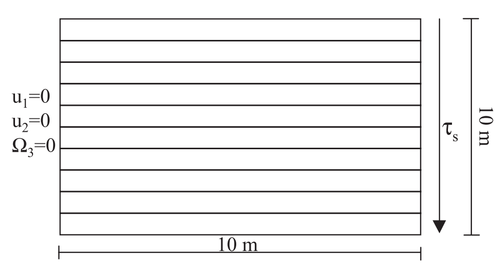

Fig. 1. A schematic of the example used in the analytical verification of the Cosserat model

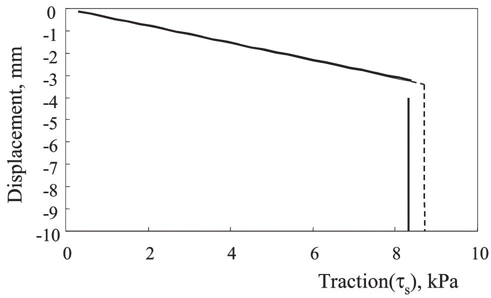

Fig. 2. Comparison of Cosserat and the analytical results. Solid line: Analytical; dotted line: Cosserat

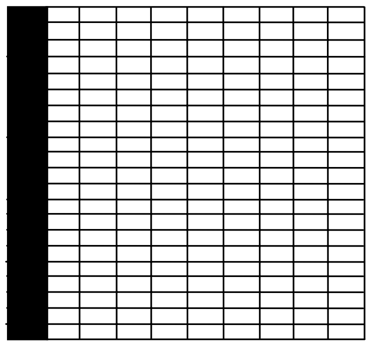

Fig. 3. Cosserat analysis result. Yielding elements are coloured black. Finite element mesh is superimposed

From the beam theory (Timoshenko and Goodier, 1970), the elastic deflection of the beam is obtained as:

$$u_2(l) = \frac{4\tau_s l^3}{Eh^2}(1 - \nu^2). \tag{22}$$

The yield stress is obtained as (Eq. 16):

$$\tau_s^{\text{yield}} = \frac{\sigma_{\text{ten}}^{\text{rock}} h}{6l}, \tag{23}$$

which gives $\tau_s^{\text{yield}} = 8.33$ kPa.

This problem is analysed with a plane strain Cosserat finite element code. The problem domain is discretized into 200 eight noded isoparametric quadrilateral elements. Figure 2 shows the comparison of the analytical and the Cosserat calculations. The elastic deflection obtained from the Cosserat model agrees quite well with the analytical deflection. The Cosserat model predicts a value of 8.73 kPa for τ_s^{yield}. The difference between the analytical and the numerical predictions are less than 5%.

In Fig. 3, the tensile yield locations in the rock layers are shown, which are located on the clamped end as predicted by the beam theory. Thus it can be seen

Table 1. Rock and joint properties obtained in the laboratory and used in the numerical analysis

Intact rock layer properties				
Young's modulus (GPa)	Poisson's ratio	cohesion (MPa)	friction angle (degree)	tensile strength (MPa)
2.2–2.6 (2.4)	0.20–0.21 (0.2)	1.4–2.6 (2.0)	34–38 (36)	1.1–1.4 (1.5 and 1.7)
Joint properties				
Cohesion (kPa)	friction angle (degree)	shear stiffness (GPa/m)	normal stiffness (GPa/m)	tensile strength
5–30 (15)	22–26 (25)	(100)	(100)	(0)

that the Cosserat model accurately predicts both the deformation and the collapse mechanism as well as collapse load of a layered medium.

A tensile stress of 72 kPa is applied on the right hand side and the above example problem is reanalysed. In this case, superposition will yield the following expression for the normal stress at the outer-fibre of the rock layer:

$$\sigma_{11}^{N} = \sigma_{\text{ten}}^{\text{rock}} = \frac{6l\iota_s^{\text{yield}}}{h} + \sigma_{11}, \quad \text{here } \sigma_{11} = 72 \text{ kPa}. \tag{24}$$

Equation (24) yields a value of $\iota_s^{\text{yield}} = 7.13$ kPa and the Cosserat model predicts a value of $\iota_s^{\text{yield}} = 6.6$ kPa.

The Cosserat finite element model is then used to back analyse a centrifuge result published previously in Adhikary et al. (1997). In that study a foliated slope model (manufactured in the laboratory from sand and gypsum) with 330 mm slope height, average layer thickness of 10 mm, layer inclination angle of 80° and slope angle of 61° was spun in a centrifuge until it failed at a g-level of about 83.

In that study, additional laboratory experiments were conducted to obtain the basic geomechanical properties of the rock layer and the joints. Table 1 summarises the laboratory results. The values shown in the parenthesis are the values adopted in the numerical calculations. The joint shear and normal stiffnesses were not measured experimentally and were assumed to be 100 GPa per meter length in the numerical calculations. This implies that the joints are practically rigid up to yielding. An average joint friction angle of 25 degree is used in the analysis. Joint dilation angle is assumed to be zero. The experimentally measured joint cohesion was found to vary from 5 kPa to 30 kPa, and this parameter is used as a fitting parameter. A number of computer simulations with different joint cohesions were carried out so that a best fit to experimental data could be obtained. The laboratory determination of tensile strength of a single 10 mm thick rock layer was found to be impractical. Hence, the tensile strength of the rock matrix in (Adhikary et al., 1997) was determined by five point bending tests on a much larger rectangular 50 mm by 50 mm beam of 300 mm length. In Adhikary et al. (1997), no attempt was made to study the sample size effect on measured tensile strength. Hence, the numerical calculations are conducted here for two different values (i.e. 1.5 MPa and 1.7 MPa) of the rock layer tensile strength.

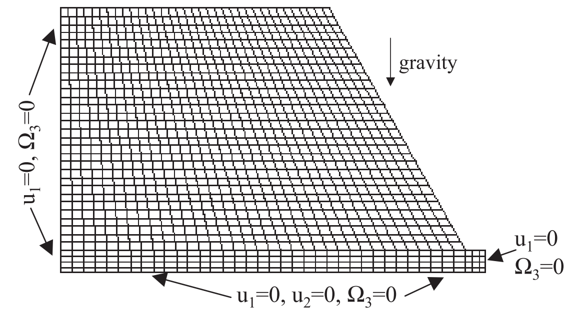

Fig. 4. The finite element mesh and the boundary conditions used in the Cosserat analysis of the centrifuge model

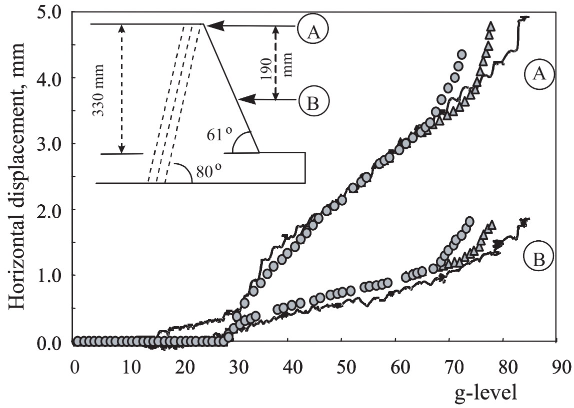

Fig. 5. Comparison of Cosserat and the centrifuge test results. Numerical calculations were conducted with rock tensile strength of 1.3 MPa and 1.5 MPa. Solid lines: experimental, data points: numerical, ●● $\sigma_t = 1.5$ MPa, ▲▲ $\sigma_t = 1.7$ MPa

Figure 4 presents the Cosserat finite element mesh and the boundary conditions used in this example. The problem was discretised using 1202 eight noded isoparametric quadrilaterals. Figure 5 presents the experimental and the numerical results obtained with a joint cohesion value of 15 kPa. It can be seen that the Cosserat model shows a very good agreement with the experimental results in terms of the failure mechanism, collapse load, and measured displacement. The model with rock layer tensile strength of 1.5 MPa predicted the slope failure at about 66 g where as the one with 1.7 MPa gave a failure g-level of about 76 compared to the experimental g-level of about 83. Figure 6 presents a plasticity plot, which shows location of rock layer tensile failure. A similar pattern of tensile cracking of rock layers was seen in the centrifuge (Adhikary et al., 1997).

4. Conclusions

A fully elasto-plastic Cosserat model, which in contrast to the earlier Cosserat models considered the possibility of rock layer plasticity in addition to joint plas-

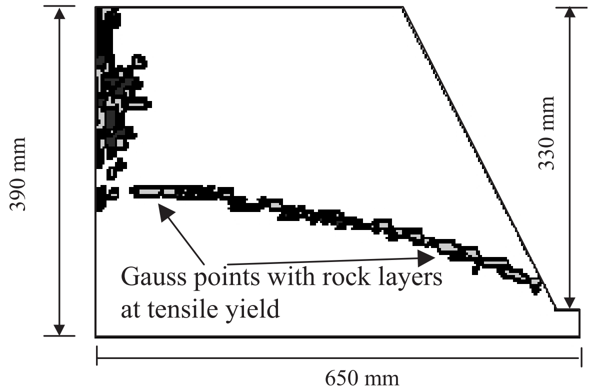

Fig. 6. Cosserat analysis result showing the rock yield

ticity, is developed. The rock layer plasticity is formulated on the basis of the symmetric part of the stress tensor with the incorporation of moment stresses. The Cosserat model is verified against an analytical solution. It is found that both the deformation and the rock failure load predicted by the Cosserat model is in very good agreement with the analytical solutions with differences of around 5%. The Cosserat model is further used to back analyse a centrifuge experiment conducted on a small scale foliated rock slope model manufactured in a laboratory. It can be seen that the predictions obtained from the Cosserat model for the slope displacement, the failure mechanism and failure load are in very good agreement with those observed in the centrifuge experiment.

Acknowledgement

The authors would like to express their sincere thanks to M. Kelly of CSIRO for his encouragement and on going support for this work. The authors are grateful to M. Kelly, S. Craig and B. Shen of CSIRO for reviewing the paper and providing valuable suggestions.

References

Adhikary, D. P., Dyskin, A. V. (1998): A continuum model of layered rock masses with non-associative joint plasticity. Int. J. Numer. Anal. Methods Geomech. 22 (4), 245–261.

Adhikary, D. P., Dyskin, A. V., Jewell, R. J., Stewart, D. P. (1997): A study of the mechanism of flexural toppling failure of rock slopes. Rock Mech. Rock Engng. 30 (2), 75–93.

Cosserat, E., Cosserat, F. (1909): Théorie des corps deformables. Hermann, Paris.

Cundall, P. A. (1987): Distinct element models of rock and soil structures. In: Brown, E. T. (ed.) Analytical and computational methods in engineering rock mechanics. Allen and Unwin, London, 129–163.

Goodman, R. E., Taylor, R. L., Brekke, T. (1968): A model for the mechanics of jointed rock. J. Soil Mech. Found. Div., Proc. ASCE 94, 637–659.

Mühlhaus, H.-B. (1993): Continuum models for layered and blocky rock. In: Comprehensive rock engineering. Invited Chapter for Vol. II, Analysis and design methods. Pergamon Press, 209–230.

Owen, D. R. J., Hinton, E. (1980): Finite elements in plasticity, theory and practice. Pineridge Press Ltd., Swansea, U.K., pp. 594.

Timoshenko, S. P., Goodier, J. N. (1970): Theory of elasticity. McGraw-Hill, New York, pp. 567.

Authors' address: Dr. Deepak Adhikary, Exploration and Mining, Queensland Centre for Advandced Technics, CSIRO, P.O. Box 883, Kenmore, Qld 4069, Australia. E-mail: deepak.adhikary@csiro.au